Validation of the Surface Daytime Net Radiation Product From Version 4.0 GLASS Product Suite

Bo Jiang, Shunlin Liang, Aolin Jia, Jianglei Xu, Xiaotong Zhang, Zhiqiang Xiao, Xiang Zhao, Kun Jia, and Yunjun Yao

***Abstract*— The daytime surface net radiation (R_n) product from version 4.0 Global LAnd Surface Satellite (GLASS) product suite was recently generated from Moderate Resolution Imaging Spectroradiometer data. It is the daytime average product of R_n derived from 2000 to 2015 at a spatial resolution of 0.05°. This letter describes the results of validation of this new R_n product using ground measurements collected from 142 sites distributed worldwide. The overall accuracy of the GLASS daytime R_n product was satisfactory, with an R^2 of 0.80, root-mean-square error of 51.35 Wm^{-2}, and mean bias error of 0.11 Wm^{-2}. Its accuracy and quality were highly consistent for different land cover classes and elevation zones.**

***Index Terms*— Global LAnd Surface Satellite (GLASS), net radiation, product, remote sensing.**

I. Introduction

THE net all-wave surface radiation (R_n), which characterizes the available radiative energy on the earth's surface, is the difference between total upward and downward radiation. R_n drives the processes of evapotranspiration, air, and soil heat fluxes, and other smaller energy-consuming processes such as photosynthesis. It also controls the exchange of energy and water between the biosphere and the atmosphere, and has a major influence on the earth's weather and climate [1]. Thus, a method to reliably measure the spatial and temporal R_n is needed. However, measurements of R_n are scarce [6], and its spatial variation thus far remains uncharacterized. An alternative method involves obtaining values of R_n from reanalysis and satellite products.

Manuscript received July 11, 2018; revised September 2, 2018, October 17, 2018, and October 18, 2018; accepted October 18, 2018. Date of publication November 19, 2018; date of current version March 25, 2019. This work was supported by the National Key Research and Development Program of China (No. 2016YFA0600101) and in part by the National Basic Research Program of China (No. 2015CB953701). *(Corresponding author: Bo Jiang.)*

B. Jiang, J. Xu, X. Zhang, Z. Xiao, X. Zhao, K. Jia, and Y. Yao are with the State Key Laboratory of Remote Sensing Science, Beijing Normal University, Beijing 100875, China, with the Institute of Remote Sensing and Digital Earth, Chinese Academy of Sciences, Beijing 100875, China, and also with the Faculty of Geographical Science, Beijing Engineering Research Center for Global Land Remote Sensing Products, Institute of Remote Sensing Science and Engineering, Beijing Normal University, Beijing 100875, China (e-mail: bojiang@bnu.edu.cn; jianglei_yx@163.com; xtngzhang@bnu.edu.cn; zhqxiao@bnu.edu.cn; zhaoxiang@bnu.edu.cn; jiakun@bnu.edu.cn; boyyunjun@163.com).

S. Liang is with the Department of Geographical Sciences, University of Maryland, College Park, MD 20742 USA, and also with the School of Remote Sensing Information Engineering, Wuhan University, Wuhan 430072, China (e-mail: sliang@umd.edu).

A. Jia is with the Department of Geographical Sciences, University of Maryland, College Park, MD 20742 USA (e-mail: aolin@terpmail.umd.edu).

Color versions of one or more of the figures in this letter are available online at http://ieeexplore.ieee.org.

Digital Object Identifier 10.1109/LGRS.2018.2877625

TABLE I
Summary of Available R_n Products

Product	Spatial Resolution	Temporal Resolution	Period	Reference
Reanalysis products				
NCEP/CFSR	T382 (38 km)	6 hourly	1979–2010	[2]
NASA/MERRA	$1/2° \times 2/3°$	1 hourly	1979–present	[3]
ERA40	T159 (125 km)	6 hourly	1957–2002	[4]
ERA-Interim	T255 (80 km)	3 hourly	1980–present	[5]
JRA55	T319 (~ 55 km)	3 hourly	1958–present	[8]
NCEP-DOE R2	T62 (200 km)	6 hourly	1979–present	[22]
Satellite products				
CERES-SYN	1°	3 hourly	2000–present	[24]
GEWEX-SRB	1°	3 hourly	1983–2007	[26]
ISCCP-FD	280 km	8day	1983–2012	[30]
MODIS-TERRA	0.05°	daily	2001-2009	[35]
GLASS-MODIS	0.05°	daytime	2000–2015	[33]

Table I lists several currently available R_n products. Reanalysis products are usually derived by merging available observations with atmospheric models to obtain the best estimate of states of the atmosphere and the surface of the land, and satellite products are generally based on a radiative transfer model with atmospheric and surface parameters as inputs. These reanalysis products usually last long time periods and have high temporal resolutions, but their accuracies were discrepancies over different regions [23]. Although satellite products are thought to be more accurate than the reanalysis products in R_n [28], their spatial resolution is too coarse to meet some requirements of scientific research and applications. Moreover, a significant anomaly was found in the latest Clouds and the Earth's Radiant Energy System (CERES) product owing to the changes in different versions of input data [29]. The daytime product R_n of the Global LAnd Surface Satellite (GLASS), derived from Moderate Resolution Imaging Spectroradiometer (MODIS) data (denoted by GLASS-MODIS), is a novel remotely sensed product. It is the only product that provides R_n as an integral variable directly, which reduces the magnitude of error accumulations from components, whereas all other products derive R_n by combining four radiative components (downward and upward shortwave and longwave radiations). Both GLASS-MODIS and MODIS-TERRA R_n products have the same spatial resolution over all other products (0.05°).

In this letter, ground measurements from 142 sites distributed globally collected from 2000 to 2015 were applied to validate the GLASS-MODIS daytime R_n product.

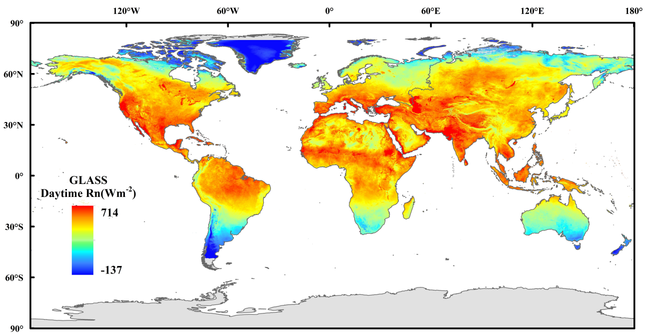

Fig. 1. Spatial explicit of GLASS-MODIS daytime R_n in June, 2003. Gray represents the missing data caused by polar night or missing inputs.

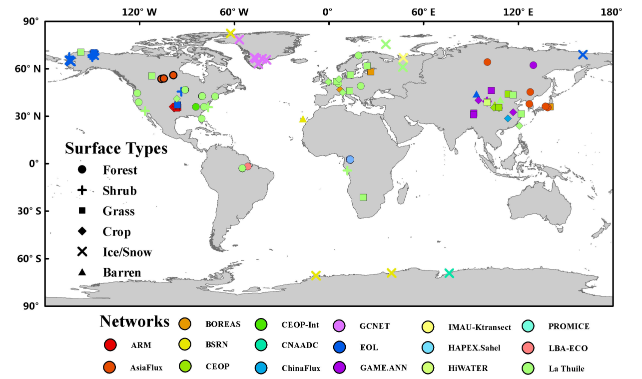

Fig. 2. Spatial distribution of 142 validation sites from 17 measurement networks. The symbols represent the land cover types of the sites. Detailed information is given in Table II.

The objective is to inform data users of the quality of this new data set.

II. GLASS-MODIS R_n Algorithm and Product

The GLASS-MODIS daytime (from sunrise to sunset) R_n product is a new time series satellite product generated from an empirical model built based on the relationship between R_n and solar radiation as well as ancillary information [33]. Following comprehensive exploration and evaluation, the multivariate adaptive regression splines (MARS) model was selected as the algorithm to use [6], [34]. The inputs for MARS included meteorological parameters (i.e., air temperature and pressure) from MERRA2 [36] and surface parameters (i.e., downward shortwave radiation (DSR) and normalized difference vegetation index (NDVI) [37]) from GLASS. The GLASS DSR data are also a new product with a spatial resolution of 0.05° at a daily scale from 2000 to 2015, generated based on a direct estimation method using top-of-the-atmosphere reflectance from MODIS, and the global validated accuracy was satisfactory with an root-mean-square error (RMSE) of 32.84 Wm^{-2} and a bias of 3.72 Wm^{-2} [38], [39]. The eight-day, 0.05° GLASS NDVI product from 2000 to 2015 was developed by Xiao *et al*. [37] using Advanced Very High Resolution Radiometer land long-term data record data, and the accuracy of this data set was confirmed to be superior to that of other products.

GLASS-MODIS R_n has a higher spatial resolution (0.05°) than most of other products, and the results of preliminary validation indicated its satisfactory accuracy [33]. Fig. 1 shows the spatial explicit of the monthly GLASS-MODIS daytime R_n in June 2003, and more details can be seen because of the high spatial resolution. At present, the GLASS-MODIS daytime R_n product is available from 2000 to 2015 to the public.

However, it is not sufficient to claim that the GLASS-MODIS daytime R_n product is reliable based only on the results of preliminary validation, and the overall quality and accuracy of the new long-term series R_n product still needs to be verified objectively.

III. Methodology

Comprehensive observations (52 176 samples) collected from 142 stations in 17 global measurement networks (Fig. 2) were used for point-based product validation. Various preprocessing and strict quality control procedures were implemented for these measurements, which were aggregated into the daytime scale [34].

Fig. 2 shows the spatial distribution of the 142 validation stations and their land cover information, and Table II gives a detailed explanation of the acronyms for all observation networks shown in Fig. 2. These validation sites were located all around the world, and even extended to the Arctic and the Antarctic regions. The various symbols represent land cover information. The elevation of these sites ranged from 1 to 2373 m above sea level. This comprehensive representation of land cover types, widespread spatial distribution, and different elevations ensured that the global applicability of the GLASS-MODIS daytime R_n product was assessed.

Three common statistical indices [R^2, RMSE, and mean bias error (MBE)] were calculated to evaluate the linear relationship between the estimates and the observed R_n. To better understand the performance of GLASS-MODIS daytime R_n under various conditions, the land cover types, elevation and cloud condition were considered for evaluation. Six common land cover classes were considered based on the land cover information obtained for each site, such as cropland, forest, grassland, shrubland, ice and snow, and barren land. Four arbitrary elevation zones were used by the validation sites (0–200, 200–500, 500–1500, and $>$ 1500 m above mean sea level). The clearness index (CI) [40] was used to determine the clear or cloud sky. The sky is defined as clear when CI > 0.9, cloudy when CI < 0.3, and mixed for other CIs.

IV. Analysis of Results

Results of the direct validation of GLASS-MODIS and CERES daytime R_n against the global validation data set are shown in Fig. 3. The scatter plots show that the overall accuracy of GLASS-MODIS daytime R_n is better than CERES with the smaller RMSE (51.35 Wm^{-2}) and MBE (0.11 Wm^{-2}). It is also found that the GLASS-MODIS modeled the daytime R_n very well in the mid-low-value range ($<$300 Wm^{-2}), but has a tendency to underestimate R_n at high values. CERES is usually taken as one of the most

TABLE II
INFORMATION CONCERNING THE 17 MEASUREMENT NETWORKS

Network/ Program	Instrument	Temporal resolution	URL
Global Fluxnet (La Thuile dataset)	Kipp&ZonenCNR-1, etc.	30 minute	http://www.fluxdata.org/
ARM	Kipp&Zonen CNR-1	10 minute	https://www.arm.gov/
AsiaFlux	Kipp&Zonen CNR-1	30 minute	http://www.asiaflux.net/
BSRN	Eppley, PIR / Kipp&Zonen CG4	1 minute	http://www.bsrn.awi.de/
BOREAS	Kipp&Zonen CM-5	30 minute	http://daac.ornl.gov/BOREAS/bhs/BOREAS_Home.html
CNAADC	Kipp & Zonen CNR1	10 minute	http://www.chinare.org.cn/
CEOP-Int	Eppley, PIR/Kipp&Zonen CG4	30 minute	http://www.eol.ucar.edu/projects/ceop/
CEOP	\	30 minute	\
ChinaFlux	Kipp & Zonen CNR-1	30/60 minute	http://www.chinaflux.org/index.aspx
EOL	Kipp & Zonen pyrgeometers, Eppley	30/60 minute	https://data.eol.ucar.edu/
GAME.ANN	EKO MS0202F	30 minute	http://aan.suiri.tsukuba.ac.jp/aan.html
GCNET	Li Cor Photodiode & REBS Q* 7	1 hourly	http://cires.colorado.edu/science/groups/steffen/gcnet/
HAPEX-Sahel	pyrradiometer 8111, REBS Q*6	10/20 minute	http://www.cesbio.ups-tlse.fr/hapex/
HiWATER	Kipp & Zonen CNR-1/CNR-4	10 minute	http://hiwater.westgis.ac.cn/
LBA-ECO	Kipp & Zonen CG2/CNR-1	30 minute	https://daac.ornl.gov/cgi-bin/dataset_lister.pl?p=11
IMAU-Ktransect	Kipp & Zonen CNR-1	60 minute	http://www.projects.science.uu.nl/iceclimate/aws/greenland.php
PROMICE	Kipp & Zonen CNR-1/CNR-4	10 minute	http://promice.org/WeatherStations.html

ARM: Atmospheric Radiation Measurement, BSRN: Baseline Surface Radiation Network [7], BOREAS: Boreal Ecosystem-Atmosphere Study, CNAADC: Chinese National Arctic and Antarctic Data Center, CEOP-Int.: Coordinated Enhanced Observing Period, CEOP: Coordinated Enhanced Observation Network of China [9, 10], EOL: Earth Observing Laboratory [11-21], GAME.ANN: GEWEX Asian Monsoon Experiment , GCNET: Greenland Climate Network [25], HAPEX-Sahel: Hydrology-Atmosphere Pilot Experiment in the Sahel [27], HiWATER: Heihe Watershed Allied Telemetry Experimental Research [9], LBA-ECO: Large-scale Biosphere-Atmosphere Experiment [31, 32], IMAU-Ktransect: Institute for Marine and Atmospheric Research Ice and Climate, PROMICE: Programme for Monitoring of the Greenland Ice Sheet.

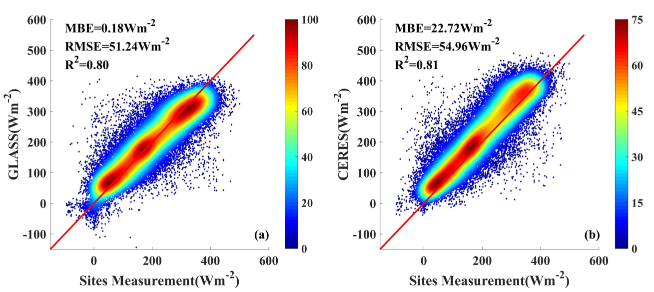

Fig. 3. Scatter plot between (a) GLASS-MODIS and (b) CERES daytime R_n and validation observations. Color bar shows point density.

reliable radiation products [23]. Comparing to GLASS, CERES generally overestimated R_n [Fig. 3(b)].

The accuracy values of GLASS-MODIS daytime R_n for various land cover types, different elevation zones and clear/cloudy conditions are given in Fig. 4 and Table III. The results in Fig. 4 and the first part of Table III indicate that the accuracy of the GLASS-MODIS daytime R_n product varied with land cover, and yielded better performance on cropland, forest, and ice and snow, with values of MBE less than that of 4.5 Wm^{-2}, whereas the largest biases were observed on grassland and shrubland, with the largest MBE of 20.21 and 23.49 Wm^{-2}, respectively. Because of the peculiarity of ice, and snow (R_n values were small), the accuracy of GLASS-MODIS was acceptable though its R^2 value is the lowest (0.68).

The results of validation by elevation zone (the second part in Table III) indicate that the relative worse performance of GLASS-MODIS daytime R_n only on low elevations

TABLE III
VALIDATION RESULTS OF GLASS-MODIS DAYTIME R_n PRODUCT (2000–2015) BY LAND COVER AND ELEVATION ZONE

Group	R^2	RMSE (Wm^{-2})	MBE (Wm^{-2})	No. of samples
I. Land Cover				
Cropland	0.84	41.11	−4.05	12,655
Forest	0.78	55.58	−4.54	28,938
Grassland	0.80	51.34	20.21	6,043
Shrubland	0.77	48.58	23.49	2,079
Ice / Snow	0.68	51.16	0.19	1,691
Barren land	0.73	50.41	12.61	808
II. Elevation				
< 200	0.80	52.69	9.01	16,421
> 200 to 500	0.77	53.06	−4.50	26,405
> 500 to 1500	0.84	43.60	−2.06	8,593
> 1500	0.87	43.51	1.90	756
III. Clear / Cloud				
0 < CI < 0.3	0.71	64.89	1.32	6,352
0.3 < CI < 0.9	0.79	52.06	4.41	30,789
0.9 < CI < 1	0.81	42.33	−8.82	15,247

(<200 m) yielding the largest RMSE (52.69 Wm^{-2}) and MBE (9.01Wm^{-2}). Across other elevation zones, GLASS-MODIS daytime R_n showed robust and consistent performance even for the range of high elevation zones (>1500 m) with an R^2 of 0.87, an RMSE of 43.51 Wm^{-2}, and an MBE of 1.90 Wm^{-2}. GLASS-MODIS tended to overestimate R_n in areas lower than 200 m above sea level. The third part in Table III shows that the accuracies of GLASS-MODIS daytime R_n under different clear or cloudy conditions were relative robust. GLASS-MODIS daytime R_n has the smallest

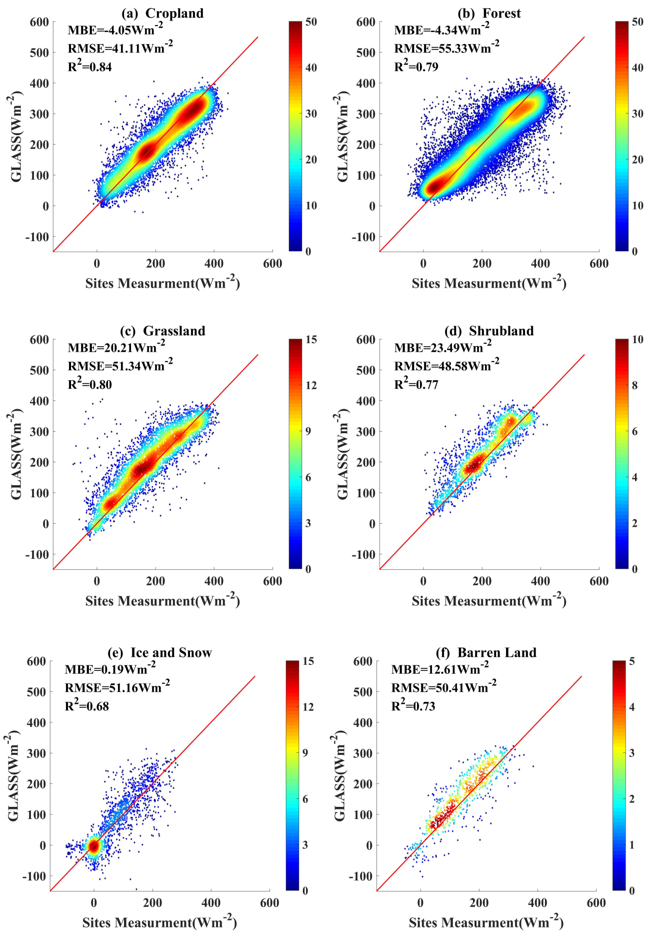

Fig. 4. Validation results of GLASS-MODIS daytime R_n product (2000–2015) aggregated into six common land cover classes. (a) Cropland. (b) Forest. (c) Grassland. (d) Shrubland. (e) Ice and snow. (f) Barren land. Color bars show point density.

RMSE (42.33 Wm^{-2}) but the largest bias (-8.82 Wm^{-2}) in clear sky, while the largest RMSE (64.89 Wm^{-2}) and the smallest bias (1.32 Wm^{-2}) in cloudy sky.

However, it should be noted that the numbers of validation observations for some land cover classes (such as ice and snow, and barren land) and high elevation areas (>1500 m) were small, which means that further validation studies are needed, by including more observations for such situations, for a more meaningful evaluation.

To check the variations in the GLASS-MODIS daytime R_n product in a long time series, two sites from ARM and La Thuile networks taken as examples are presented in Fig. 5.

From the two plots, it is evident that GLASS-MODIS captured the variations in daytime R_n measurements in the long time series very well, and the corresponding statistical values of each site (shown on top of each plot) verified the accuracy of the GLASS-MODIS daytime R_n product. However, it is also found that GLASS-MODIS tends to overestimate R_n in low values of R_n and underestimate R_n in large values of R_n.

Overall, the above results show that the GLASS-MODIS daytime R_n product delivers satisfactory performance in daytime R_n estimation for various land cover types and elevation zones from 2000 to 2015, and captures variations in daytime R_n well for long time periods.

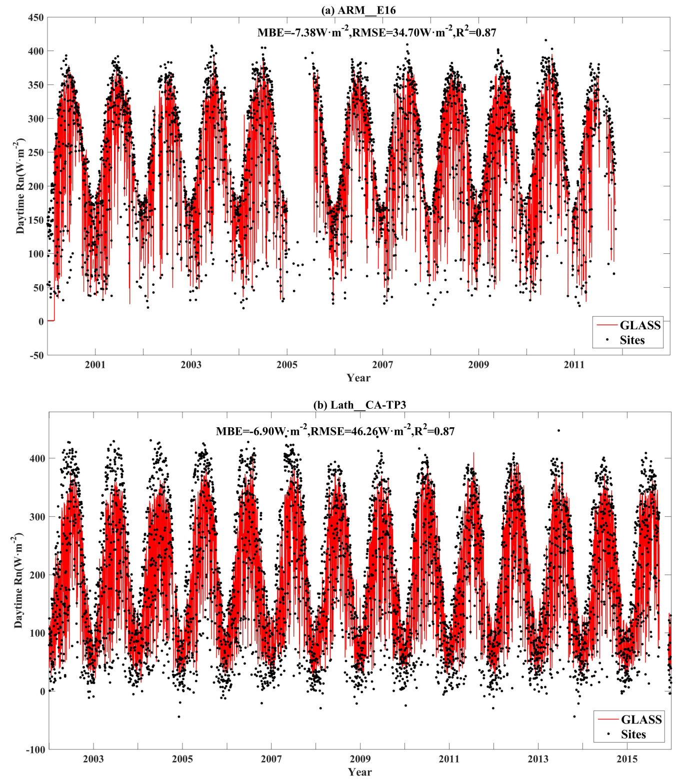

Fig. 5. Time series of GLASS-MODIS daytime R_n product (red line) and observations (black spots) from two sites. (a) ARM_E16 (36.06° N, 99.13° W, Cropland). (b) Lath_CA-TP3 (42.71° N, 80.35° W, evergreen needle-leaf forest).

V. SUMMARY

We recently developed the first global high-resolution (0.05°) temporally continuous daytime R_n satellite product GLASS-MODIS. Before its use by the scientific community, it is important to quantify its accuracy. This letter reported results of the validation results of the GLASS-MODIS daytime R_n product from 2000 to 2015 by a comprehensive global observation data set. The validation was conducted by directly comparing with measurements in R_n, which were then grouped into six common land cover types (cropland, forest, grassland, shrubland, ice and snow, and barren land), four elevation zones (<200, 200–500, 500–1500, and >1500 m) and clear/cloudy skies ($0.9 < CI < 1$, $0.3 < CI < 0.9$, and $CI < 0.3$). The results of the validation indicated that the overall accuracy of the GLASS-MODIS daytime R_n product (2000 to 2015) is satisfactory and better than CERES, with an R^2 of 0.80, an RMSE of 51.35 Wm^{-2}, and an MBE of 0.11Wm^{-2}. For most land cover types, the performance of the GLASS-MODIS R_n was robust, even for special land cover classes such as ice and snow. Regarding elevation, the accuracy of GLASS-MODIS R_n was a little bit lower in low elevation zones (<200 m), whereas its performance was consistent for other elevation zones. The performance of GLASS-MODIS R_n was also robust for different sky conditions. Two examples were provided to highlight the impressive capability of GLASS-MODIS to capture variations in the daytime R_n values for a long time series. Furthermore, its high spatial resolution can provide details that can benefit other applications. However, there are deficiencies in this study of the GLASS-MODIS daytime R_n product, either due to the algorithm within the package or the input data. It is also worth noting that the direct validation results shown in this letter from using the "point" measurements are valid only if the atmospheric and surface conditions are homogeneous, and more validation works addressing the scaling issue should be conducted. Further validation and experiments should thus be carried out to improve the GLASS-MODIS daytime R_n product in the future research.

In summation, the GLASS-MODIS daytime R_n product with a spatial resolution of 0.05°, for data from 2000 to 2015, is reliable with a satisfactory accuracy, and has significant potential for wide use in the near future. The GLASS-MODIS daytime R_n product is freely available to the public at http://glass-product.bnu.edu.cn/introduction/allwave.html.

ACKNOWLEDGMENT

This work used eddy covariance data acquired by the FLUXNET community. The authors would like to thank Dr. Y. Li and Dr. R. Li from the Xinjiang Institute of Ecology and Geography, CAS, Beijing, China, and Dr. J. C. Calvet from CNRM-GAME for sharing their data.

REFERENCES

[1] M. Wild *et al.*, "The energy balance over land and oceans: An assessment based on direct observations and CMIP$_5$ climate models," *Climate Dyn.*, vol. 44, pp. 3393–3429, Jun. 2015.

[2] S. Saha *et al.*, "The NCEP climate forecast system version 2," *J. Climate*, vol. 27, no. 6, pp. 2185–2208, 2013.

[3] M. M. Rienecker *et al.*, "MERRA: NASA's Modern-Era Retrospective Analysis for Research and Applications," *J. Climate*, vol. 24, pp. 3624–3648, Jul. 2011.

[4] S. M. Uppala *et al.*, "The ERA-40 re-analysis," *Quart. J. Roy. Meteorol. Soc.*, vol. 131, no. 612, pp. 2961–3012, 2005.

[5] D. P. Dee *et al.*, "The ERA-Interim reanalysis: Configuration and performance of the data assimilation system," *Quart. J. Roy. Meteorol. Soc.*, vol. 137, pp. 553–597, Apr. 2011.

[6] B. Jiang, Y. Zhang, S. Liang, X. Zhang, and Z. Xiao, "Surface daytime net radiation estimation using artificial neural networks," *Remote Sens.*, vol. 6, no. 11, pp. 11031–11050, 2014.

[7] A. Ohmura *et al.*, "Baseline surface radiation network (BSRN/WCRP): New precision radiometry for climate research," *Bull. Amer. Meteorol. Soc.*, vol. 79, no. 10, pp. 2115–2136, 1998.

[8] S. Kobayashi *et al.*, "The JRA-55 reanalysis: General specifications and basic characteristics," *J. Meteorol. Soc. Jpn.*, vol. 93, no. 1, pp. 5–48, 2015.

[9] S. M. Liu *et al.*, "A comparison of eddy-covariance and large aperture scintillometer measurements with respect to the energy balance closure problem," *Hydrol. Earth Syst. Sci.*, vol. 15, pp. 1291–1306, Apr. 2011.

[10] Z. Xu *et al.*, "Intercomparison of surface energy flux measurement systems used during the HiWATER-MUSOEXE," *J. Geophys. Res. Atmos.*, vol. 118, no. 23, pp. 13140–13157, Dec. 2013.

[11] F. III, W. Eugster, and J. McFadden, "Eddy flux data, alaska north slope, 1994–1996, Version 1.0," UCAR/NCAR-Earth Observing Laboratory, 2009.

[12] L. Hinzman, "Council radiation data—Station C1. Version 1.0," UCAR/NCAR-Earth Observing Laboratory, 2007.

[13] L. Hinzman, "Council radiation data—Station C3. Version 1.0," UCAR/NCAR-Earth Observing Laboratory, 2007.

[14] L. Hinzman, "Kougarok radiation data—Station K1. Version 1.0," UCAR/NCAR-Earth Observing Laboratory, 2007.

[15] L. Hinzman, "Kougarok radiation data—Station K2. Version 1.0," UCAR/NCAR-Earth Observing Laboratory, 2007.

[16] L. Hinzman, "Kougarok radiation data—Station K3. Version 1.0," UCAR/NCAR-Earth Observing Laboratory, 2007.

[17] J. Marengo, "LBA: Santarem surface meteorology and radiation data set. Version 1.0," UCAR/NCAR-Earth Observing Laboratory, 2011.

[18] O. Hartogensis, "Radiation, THP and soil sensor 10-min data. Version 1.0," UCAR/NCAR-Earth Observing Laboratory, 2006.

[19] J. Baker, "GCIP/ESOP-98 surface: Waseca, MN surface meteorological and radiation data. Version 1.0," UCAR/NCAR-Earth Observing Laboratory, 1998.

[20] J. Randerson and H. Liu, "Growing season energy and CO_2 fluxes over a larch forest tundra ecosystem in siberia, version 1.0," UCAR/NCAR-Earth Observing Laboratory, 2009.

[21] J. Baker, "GCIP/ESOP-97 surface: Rosemount, MN surface meteorological and radiation data. Version 1.0," UCAR/NCAR-Earth Observing Laboratory, 1998.

[22] M. Kanamitsu *et al.*, "NCEP–DOE AMIP-II reanalysis (R–2)," *Bull. Amer. Meteorol. Soc.*, vol. 83, no. 11, pp. 1631–1643, 2002.

[23] A. Jia *et al.*, "Comprehensive assessment of global surface net radiation products and uncertainty analysis," *J. Geophys. Res.-Atmos.*, vol. 123, pp. 1970–1989, Feb. 2018.

[24] B. A. Wielicki *et al.*, "Clouds and the Earth's Radiant Energy System (CERES): Algorithm overview," *IEEE Trans. Geosci. Remote Sens.*, vol. 36, no. 4, pp. 1127–1141, Jul. 1998.

[25] K. Steffen *et al.*, "Greenland climate network (GC-Net)," US Army Cold Regions Reattach Eng. (CRREL), Tech. Rep., 1996, pp. 98–103.

[26] P. W. Stackhouse *et al.*, The WCRP/GEWEX surface radiation budget project release 2: An assessment of surface fluxes at 1 degree resolution," in *Proc. Int. Radiat. Symp.*, St. Petersburg, Russia, 2001.

[27] S. D. Prince *et al.*, "Geographical, biological and remote sensing aspects of the Hydrologic Atmospheric Pilot Experiment in the Sahel (HAPEX-Sahel)," *Remote Sens. Environ.*, vol. 51, no. 1, pp. 215–234, Jan. 1995.

[28] S. Liang, K. Wang, X. Zhang, and M. Wild, "Review on estimation of land surface radiation and energy budgets from ground measurement, remote sensing and model simulations," *IEEE J. Sel. Topics Appl. Earth Observ. Remote Sens.*, vol. 3, no. 3, pp. 225–240, Sep. 2010.

[29] L. J. Cheng, K. E. Trenberth, J. Fasullo, T. Boyer, J. Abraham, and J. Zhu, "Improved estimates of ocean heat content from 1960 to 2015," *Sci. Adv.*, vol. 3, no. 3, p. e1601545, Mar. 2017.

[30] W. B. Rossow and Y.-C. Zhang, "Calculation of surface and top of atmosphere radiative fluxes from physical quantities based on ISCCP data sets: 2. Validation and first results," *J. Geophys. Res.-Atmos.*, vol. 100, no. D1, pp. 1167–1197, Jan. 1995.

[31] S. D. Miller, M. L. Goulden, and H. R. Da Rocha, "LBA-ECO CD-04 meteorological and flux data, Km 83 tower site, Tapajos national forest," Ornl Distributed Active Archive Center, 2009.

[32] S. R. Saleska, H. R. Da Rocha, A. R. Huete, A. D. Nobre, P. E. Artaxo, and Y. E. Shimabukuro, "LBA-ECO CD-32 flux tower network data compilation, Brazilian Amazon: 1999–2006," Ornl Distributed Active Archive Center, 2013.

[33] B. Jiang *et al.*, "GLASS daytime all-wave net radiation product: Algorithm development and preliminary validation," *Remote Sens.*, vol. 8, no. 3, p. 222, 2016.

[34] B. Jiang *et al.*, "Empirical estimation of daytime net radiation from shortwave radiation and ancillary information," *Agricult. Forest Meteorol.*, vols. 211–212, pp. 23–36, Oct. 2015.

[35] M. Verma *et al.*, "Global surface net-radiation at 5 km from MODIS Terra," *Remote Sens.*, vol. 8, no. 9, p. 739, 2016.

[36] R. Gelaro *et al.*, "The Modern-Era Retrospective Analysis for Research and Applications, version 2 (MERRA-2)," *J. Climate*, vol. 30, pp. 5419–5454, Jul. 2017.

[37] Z. Xiao, S. Liang, X. Tian, K. Jia, Y. Yao, and B. Jiang, "Reconstruction of long-term temporally continuous NDVI and surface reflectance from AVHRR data," *IEEE J. Sel. Topics Appl. Earth Observ. Remote Sens.*, vol. 10, no. 12, pp. 5551–5568, Dec. 2017.

[38] X. T. Zhang, S. Liang, G. Zhou, H. Wu, and X. Zhao, "Generating global LAnd surface satellite incident shortwave radiation and photosynthetically active radiation products from multiple satellite data," *Remote Sens. Environ.*, vol. 152, pp. 318–332, Sep. 2014.

[39] X. Zhang, S. Liang, G. Zhou, H. Wu, and X. Zhao, "Generating Global LAnd Surface Satellite incident shortwave radiation and photosynthetically active radiation products from multiple satellite data," *Remote Sens. Environ.*, vol. 152, pp. 318–332, Sep. 2014.

[40] M. G. Iziomon, H. Mayer, and A. Matzarakis, "Empirical models for estimating net radiative flux: A case study for three mid-latitude sites with orographic variability," *Astrophysics Space Sci.*, vol. 273, nos. 1–4, pp. 313–330, 2000.